Use of Paramagnetic Probes for the Study of Liquid Adsorbed on Porous Supports. Copper(II) in Water Solution

Valerio Bassetti, Leo Burlamacchi, and Giacomo Martini*

Contribution from the Istituto di Chimica Fisica, Università di Firenze, 50121 Firenze, Italy. *Received January 26, 1979*

Abstract: The electron spin resonance of $Cu(H_2O)_6^{2+}$ ion in aqueous solution adsorbed on silica gels with pore diameters in the range 4–100 nm has been used in connection with differential scanning calorimetry for the study of solid–liquid interaction. The line-shape analysis above room temperature made it possible to establish that adsorbed water behaves in the same manner as bulk water in supports with pore diameter ≥ 10 nm, while a decreased mobility was observed below this value. This fact was attributed to a different degree of immobilization of the water layers to the innermost ones. From both ESR and DSC, two different types of water were recognized with freezing: (1) unfreezable water, which is confined to the first eight to ten layers of water molecules, in which the usual ice structure cannot be formed because of the different structure of water due to the surface interaction; (2) freezable water, which involves the bulk water in pores larger than 4 nm, and undergoes crystallization with depressed freezing point because of long-range meniscus effects.

Introduction

The interaction between adsorbed water and solid surfaces is a problem that has received continuous attention. The properties of adsorbed water are influenced by the dynamical and structural nature of the surface.[1,2] The distance to which the surface interactions are appreciable is still the subject of considerable discussion: values that range from a few molecular diameters to 10^3 nm have been hypothesized.[1] Many techniques have been employed for such investigations, the most widely used being NMR, IR, and DTA.[3-6]

Recently, ESR of paramagnetic probes has also been used. Cu(II) ion was found to be a particularly useful probe since its ESR spectra are readily observable over a large temperature range. With respect to Mn(II) ion, which was previously used in porous supports,[7-9] Cu(II) has some advantages. Firstly, Cu(II) ions are ESR detectable even in low-symmetry environments, making structural information more reliable. For this reason Cu(II) may be usefully studied both in the liquid phase and in the solid bulk lattice. Furthermore, as two main relaxation mechanisms govern its ESR line width,[10] it can be studied in a large field of solvent viscosity without the complications arising from the inhomogeneous effects observed with Mn(II) solutions.[11]

This paper reports an ESR study of the aquo complex $Cu(H_2O)_6^{2+}$ in water solution adsorbed on porous supports with different pore size. The ESR data have been complemented with differential scanning calorimetry (DSC).

Experimental Section

Materials. Water solutions of Cu(II) at different concentrations (from 0.025 to 0.1 mol/dm^3) were prepared from a 0.2 mol/dm^3 $Cu(ClO_4)_2 \cdot 4H_2O$ (Ventron) stock solution. Variations of the pH were obtained by adding the appropriate amount of perchloric acid. Impregnation of the solid supports with the Cu(II) solution was carried out in the conventional way by putting the porous support into the solution, storing for 24 h, and then filtering. After filtration, the solid was gently dried on a filter paper until an apparently dry powder was obtained, which was stored in a water vapor saturated box in order to maintain full hydration.

The supports used are listed in Table I together with some of their physical properties.

Techniques. ESR spectra were taken with a Bruker 200tt spectrometer and sample holders were sealed quartz capillaries (1 mm i.d.). Temperature variation was obtained with the Bruker B-ST 100/700 variable temperature accessory.

DSC diagrams were obtained with a Perkin-Elmer DSC 1B differential scanning calorimeter. The usual volatile-sample pans were used. The diagrams were registered at constant rate of heating.

Optical spectra were carried out with a UV-vis Perkin-Elmer Model 200 spectrophotometer equipped with an internal reflection accessory. MgO was used as a standard.

Results and Discussion

At room temperature, fully hydrated silica samples containing Cu(II) water solution show a single ESR line centered at $g = 2.18$ (peak to peak width $\sim$140 G) whose hyperfine splitting is not resolved. This line closely resembles the one observed in a pure water solution[12,13] and it is clearly due to the $Cu(H_2O)_6^{2+}$ ions dissolved in the liquid water filling the pores.

When solutions with differing Cu(II) concentrations are adsorbed (from 0.025 to 0.1 mol/dm^3 giving a Cu/Si ratio of 0.01–0.04) the ESR signal intensities are linearly dependent on the Cu(II) concentration. Runs carried out with differing amounts of adsorbed 0.05 mol/dm^3 Cu(II) solution, in order to reach Cu/Si ratios equal to those reported above, show closely comparable ESR intensities. pH variations from 3.7 to 1.1 influence the line shape and the intensity in the same way in free and in adsorbed solutions. All this proves that no appreciable ion exchange occurs, and the adsorbed solution retains its initial concentration.

ESR Line Shape at Room Temperature and Above. Two main relaxation mechanisms govern the ESR line width in Cu(II) solutions.[10,12-15] The first is spin rotation, whose contribution is given by[16]

$$\Delta H(\mathrm{SR}) = \alpha' \approx (2\hbar/\sqrt{3}\langle g\rangle\beta_0)(\Delta g_\parallel^2 + 2\Delta g_\perp^2)/9\tau_r \quad (1)$$

This mechanism is independent of both applied field and nuclear quantum spin number. τ_r has usually been identified with the Debye reorientational correlation time[12-16]

$$\tau_r = 4\pi a^3\eta/3kT \quad (2)$$

The dependence of $\Delta H(\mathrm{SR})$ on T/η predicted by eq 1 and 2 makes the ESR line width increase with increasing temperature, so that the spin rotational mechanism dominates in the high-temperature region. The second mechanism is modulation of the g and A tensor anisotropies, whose contribution was found to be[15]

$$\Delta H(g,A) = \alpha'' + \beta m_I + \gamma m_I^2 \ldots \quad (3)$$

where

$$\alpha'' = (2\hbar/3^{1/2}\langle g\rangle\beta_0) \times \left\{\frac{1}{45}(\Delta g\beta_0 H/\hbar)^2[4\tau_c + 3\tau_c/(1+\omega_0^2\tau_c^2) + \frac{1}{24}(\Delta A/\hbar)^2[3\tau_c + 7\tau_c/(1+\omega_0^2\tau_c^2)]\right\} \quad (4)$$

0002-7863/79/1501-5471$01.00/0

Table I. Physical Properties of the Merck Adsorbent for Chromatography Used in This Work

denomination	specific surface area, m^2/g	pore diameter, nm	pore vol, cm^3/g
silica gel, S4	650	4	0.65
silica gel, S6	400	6	0.65
silica gel, S20	150	20	0.65
silica gel, S50	50	50	0.65
silica gel, S100	25	100	0.65
activated carbon	1300	0.5-1.5 (max 0.7-1)	1.25
aluminum oxide			
basic	130	8	0.27
acid	110	10	0.27

Table II. Magnetic Parameters of $Cu(H_2O)_6^{2+}$ on Porous Supports

sample	$g_\parallel$ (±0.004)	$g_\perp$ (±0.003)	$A_\parallel$, $cm^{-1} \times 10^4$ (±3)
Cu(II)-S4	2.410	2.081	147
Cu(II)-S6	2.409	2.081	149
Cu(II)-S20	2.408	2.081	149
Cu(II)-S50	2.406	2.080	150
Cu(II)-S100	2.407 ± 0.008	2.082 ± 0.005	150 ± 5
Cu(II)-activated carbon	2.379	2.078	161
$Cu(H_2O)_6^{2+}$-water/glycerol soln	2.409	2.082	144

$$\beta = (2\hbar/3^{1/2}\langle g\rangle\beta_0)\left\{\frac{2}{45}(\Delta A\Delta g H\beta_0/\hbar^2) \times [4\tau_c + 3\tau_c/(1+\omega_0^2\tau_c^2)]\right\} \quad (4a)$$

$$\gamma = \frac{1}{90}(\Delta A/\hbar)^2[5\tau_c - \tau_c/(1+\omega_0^2\tau_c^2)] \quad (4b)$$

The correlation time τ_c has been identified with the Debye reorientational time, τ_r, for heterocoordinated complexes[17-20] and with the pseudoreorientational time, τ_i, governed by the interconversion of the Jahn-Teller distortion axis, for the symmetrical complexes such as $Cu(H_2O)_6^{2+}$, $Cu(CH_3OH)_6^{2+}$, and $Cu(bpy)_3^{2+}$.[12,18,21,22]

From the above mechanisms it is expected that variations of the solvent viscosity or, more precisely, of the mobility of the solvent molecules around the paramagnetic ion can be followed from the ESR line shape. Thus, if adsorbed water decreases its mean mobility with respect to bulk water, the Cu(II) line width will decrease at high temperature and increase at low temperature.

For our purpose it is sufficient to consider the m_I independent part of the line width, i.e.

$$\Delta H(0) = \alpha' + \alpha'' \quad (5)$$

The width of each hyperfine component has been computed following the procedure described by Lewis et al.[13] Figures 1a and 1b show the $\Delta H(0)$ values of the Cu(II) solution adsorbed on S4, S6, S20, S50, and S100 as a function of the reciprocal temperature. For comparison, $\Delta H(0)$ values in pure water solution are also reported. The line-width behavior with temperature appreciably differs from that of pure water for S4 and S6 samples. No appreciable difference is observed for samples with pore diameter >6 nm.

Since α' dominates at high temperatures, it can be separated from the contribution of α''. From the magnetic parameters (obtained from frozen samples, see Table II) evaluation of τ_r is straightforward and for S4 sample a $\tau_r = 5.0\ (\pm 0.2) \times 10^{-11}$ s is obtained at 25 °C.

Because of the close similarity of $\Delta H(0)$ in S20, S50, and S100 to that of the pure water solution, it can be assumed that for Cu(II) in the water solution adsorbed on these supports the correlation times τ_r and τ_i are equal to those in a pure water solution for which τ_r and τ_i, at 25 °C, were reported to be 3.4×10^{-11} and 1.5×10^{-11} s, respectively.[21]

Assuming, as a rough simplification, pores of cylindrical shape and an effective volume of 0.03 nm^3 for the water molecule, about 400 water molecules may enter into an idealized cylindrical pore of 4-nm diameter and 1-nm length as in S4 silica. The mean number of water layers formed in the pores ranges from eight to ten and a relevant amount (>30%) of the intracrystalline water should be located in the first two layers. The decreased mobility (~1.5 times less than in pure water solution) should therefore involve almost all layers, although a different degree of water immobilization from the surface layers up to the innermost ones may be reasonably assumed to be present. The time scale of the ESR experiment is such that ions in different motional environments are time averaged to a single line only when τ_r is shorter than the electron spin relaxation time T_2. Ions with τ_r longer than T_2 relax as if they were isolated from the others.[11] Since paramagnetic probes dissolved in such liquid should experience a widespread distribution of correlation times, part of them longer than T_2, the resulting line shape must be regarded as a sum of line shapes with different widths (see also the section on the freezing properties of adsorbed water for further details on this point).

Data previously reported for a Cu(II) aqueous solution adsorbed on synthetic Y zeolites[21] gave values of 3×10^{-10} and 9.3×10^{-11} s at 25 °C for τ_r and τ_i, respectively, which correspond to a marked decrease of the liquid mean mobility as expected from the low water content in the faujasite cavity in fully hydrated Y zeolites (~28-30 molecules).[23]

In S6 silica gel about 10^3 water molecules may enter into a pore of 1-nm length giving rise to about 15 layers. About 23 and 85% of the total water content is located in the first two and ten layers, respectively. The influence of the solid substrate on the water mobility is reduced with respect to S4 as can be seen from the $\Delta H(0)$ behavior in Figure 1a.

In the wide-pore silica gels S20, S50, and S100, a huge number of water molecules may fill the idealized cylindrical cavity of 1-nm length (about 10^4, 6×10^4, and 2.5×10^5, respectively, with water layers ranging from 50 to 250). It is therefore plausible that the influence of surface effects on the

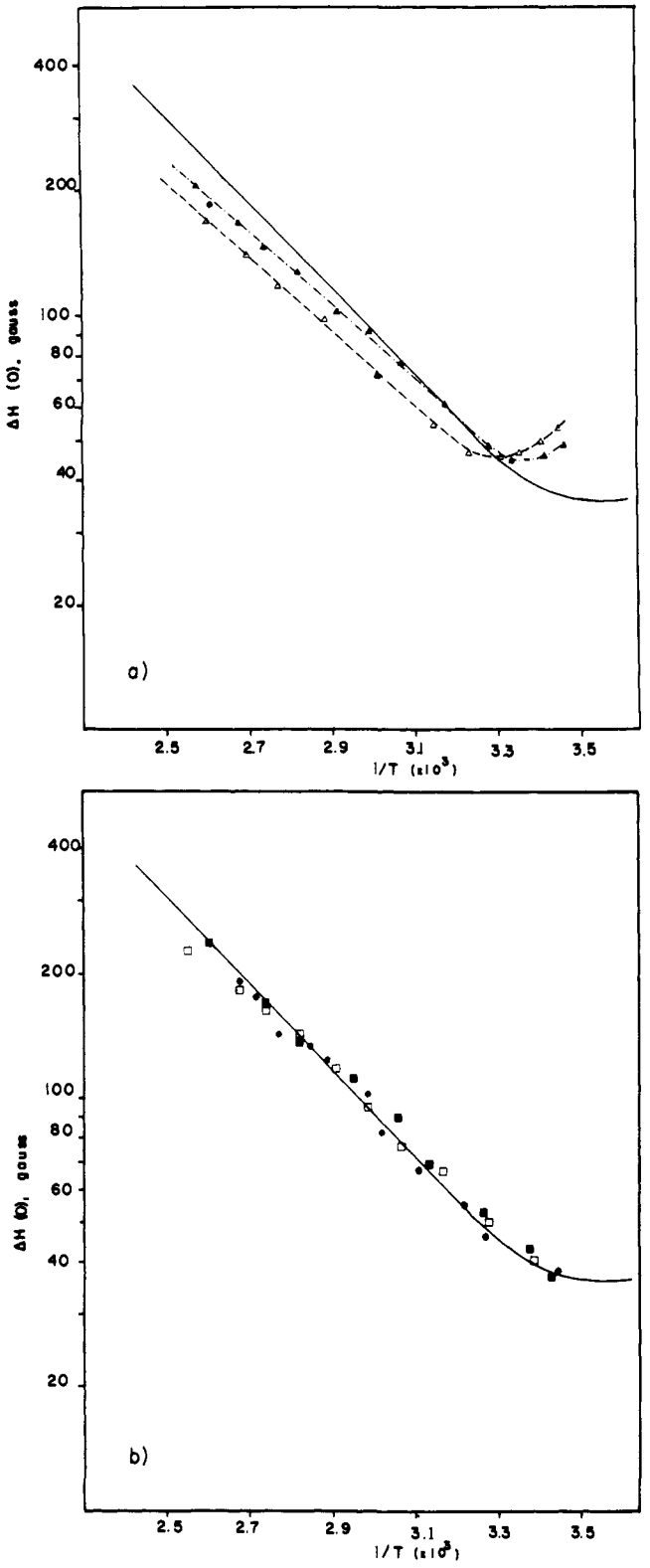

Figure 1. ESR line width $\Delta H(0)$ as a function of reciprocal temperature. Full line, $Cu(H_2O)_6^{2+}$ in unadsorbed water solution; (a) $Cu(H_2O)_6^{2+}$ water solution adsorbed on S4 (△) and S6 (▲); (b) $Cu(H_2O)_6^{2+}$ water solution adsorbed on S20 (□), S50 (■), and S100 (*).

bulk water mobility in the center of wide pores is negligible above room temperature.

Adsorption of Cu(II) solution on heteroporous carbon (pore diameter in the range 0.5–1.5 nm; see Table I) gives rise to quite different spectra in which solid- and liquid-type signals appear simultaneously (Figure 2). The widespread pore size allow only a few water molecules (up to a maximum of 60 in

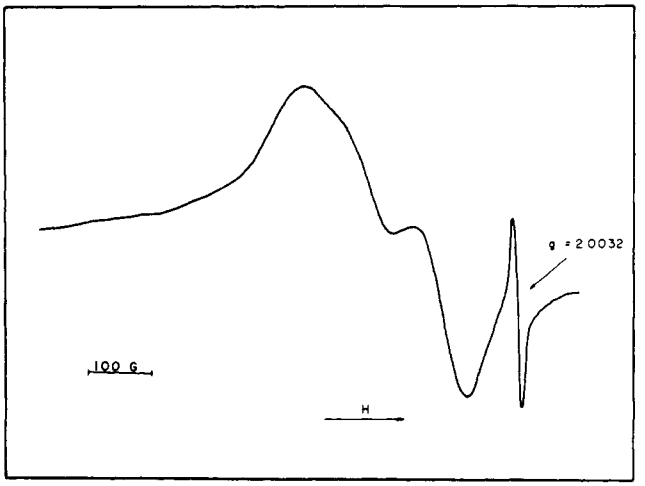

Figure 2. ESR signal from $Cu(H_2O)_6^{2+}$ water solution adsorbed on heteroporous carbon. The narrow signal at $g = 2.0032$ is due to a carbon radical ($T = 293$ K).

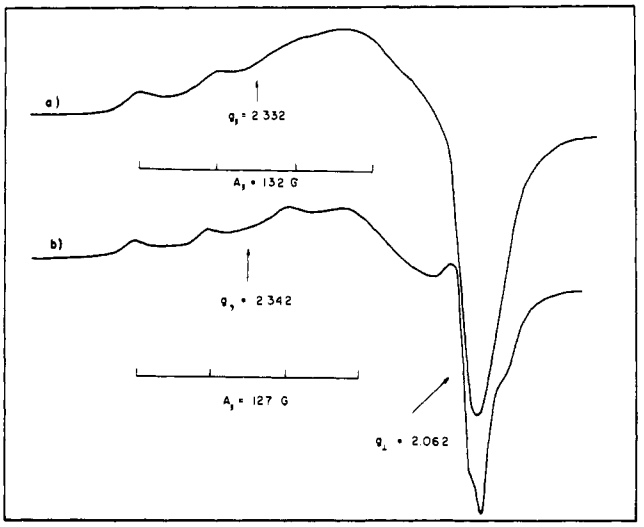

Figure 3. ESR spectra at room temperature of $Cu(H_2O)_6^{2+}$ adsorbed on basic alumina (a) and MgO (b).

the largest cavities) to enter and no more than two to three water layers can be formed. As a consequence, the mobility of Cu(II) ions must be strongly reduced, and some of them are immobilized, presumably those in the narrowest pores, giving rise to a solid-like spectrum. The Cu(II) ions far away from the surface in the largest pores still behave as in a bulk liquid environment. In principle, the liquid-type spectrum should break down and convert to a solid-type spectrum when the correlation times for the tumbling are of the order of magnitude of the reciprocal anisotropy of the spin energy.[24,25] In our case this should happen with $\tau_r \sim 10^{-8}$–10^{-9} s and with a solvent viscosity of the order of 100 cP.

Other porous supports have been investigated, namely, MgO and wide-pore acid and basic aluminas. On these systems, solid-like spectra of Cu(II) are obtained even at room temperature after adsorption of solutions of low Cu(II) concentration (Figure 3). This happens probably because of the high reactivity of the alumina and MgO surface which causes most of the Cu(II) ions to be chemisorbed on the surface, probably at specific -OH sites. No detailed information on the water mobility in these supports can be obtained from Cu(II) ESR spectra. For aluminas more detailed information was obtained by using Mn(II) as a paramagnetic probe,[7,8] that made it possible to establish that surface interactions extend up to 15–20 Å from the surface.[8]

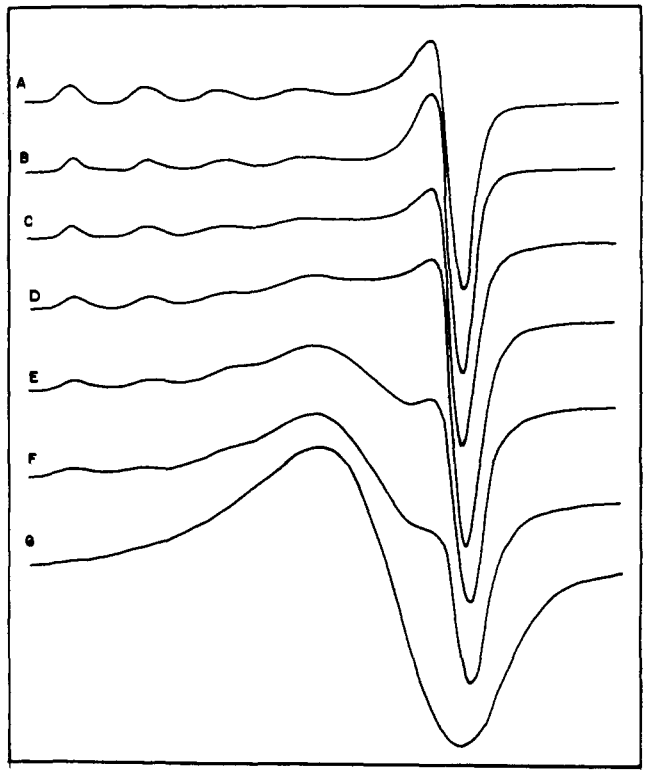

Figure 4. ESR spectra at 77 K of $Cu(H_2O)_6^{2+}$ in water-5% glycerol (A), on S4 (B), S6 (C), S20 (D), S50 (E), and S100 (F), and in bulk crystallized water (G).

ESR Spectra at Liquid Nitrogen Temperature. Figure 4 shows the frozen ESR spectra (at 77 K) of Cu(II) on S4, S6, S20, S50, and S100 together with those in bulk water-5% glycerol glass and in bulk crystallized water. The spectrum in pure water (spectrum G) is broad and unresolved. This is clearly due to the fact that, upon crystallization, a heterogeneous mixture of ice and copper salt crystals tends to form. In the presence of glycerol, the ice structure cannot be formed and the copper ions, upon cooling, are quenched in a glassy matrix into dispersed sites equivalent to those occupied in the liquid. Thus, the ESR spectrum retains its structural features with resolved hyperfine structure (hfs) components (spectrum A). The hfs components, which are well resolved in the bulk glass and in the S4 samples (spectra A and B), become less resolved with increasing pore diameter, and are completely unresolved in crystallized water (spectrum G). In fact, spectra C, D, E, and F can be interpreted as the superimposition of spectra A and G with different relative weights.

Figure 5 shows the ESR signal at 77 K of Cu(II) on carbon; a good resolution of the axial anisotropies is observed.

Table II reports the magnetic parameters of the axially resolved ESR spectra from the various supports. The ESR parameters of Cu(II) in the frozen state on silica gels do not appreciably differ from those of $Cu(H_2O)_6^{2+}$ in water-glycerol glass. All signals are interpretable in terms of the spin Hamiltonian for d^9 ions in axial symmetry

$$\mathcal{H} = g_{\parallel}\beta H_z S_z + g_{\perp}\beta[S_x H_x + S_y H_y] + A_{\parallel} I_z S_z + A_{\perp}[I_x S_x + I_y S_y] \quad (6)$$

where the symbols have their usual meaning. The bonding coefficients can be evaluated from the magnetic parameters and the transition energies with various procedures.[26,27] The small differences observed in the parameters themselves show that the $Cu(H_2O)_6^{2+}$ complexes responsible for the axially resolved spectra are only slightly but significantly influenced by the interaction with the pore surface. Also the transition

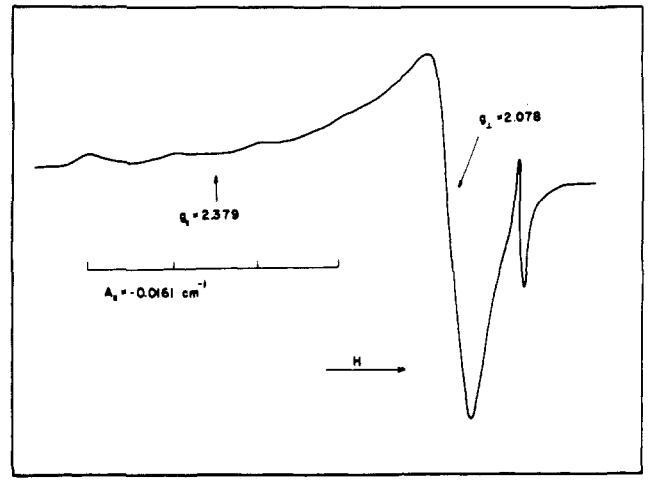

Figure 5. ESR spectra of $Cu(H_2O)_6^{2+}$ aqueous solution adsorbed on heteroporous carbon (T = 77 K).

energies obtained from optical spectra of the fully hydrated silica samples at room temperature are only slightly higher (12 900–13 000 cm^{-1}) than the 12 660-cm^{-1} transition of $Cu(H_2O)_6^{2+}$ in water solution. Opposite to aluminas and MgO, the linking of Cu(II) on the bonding groups of the surface (such as -OH groups) can be ruled out even at low temperature.

In carbon, larger $A_{\parallel}$ and lower $g_{\parallel}$ values are obtained. This trend occurs when Cu(II) complexes undergo elongation of the octahedral symmetry toward the square-planar symmetry.[28] It seems unlikely that this fact would find its explanation in the adsorption on surface sites because of the nonpolar nature of the carbon. Variations in the structure of water in the pores (see next section) may justify this finding.

Freezing Properties of Adsorbed Water. We will now discuss the freezing properties of water adsorbed on porous supports as they can be deduced from ESR and calorimetric data.

Figure 6 shows the ESR spectra of Cu(II) on S4 with decreasing temperature from 20 to −100 °C. At 10 °C the hfs structure appears and has its best resolution between −20 and −30 °C. Below this temperature the line width increases again as predicted by the relaxation mechanisms outlined above. With decreasing temperature, the axial spectrum typical of a glassy matrix (signal A of Figure 4) acquires intensity and below −70 °C the liquid spectrum disappears. Surprisingly enough, this solid-type spectrum is observable even at room temperature (as a background signal flanking the high-field side of the liquid spectrum). The simultaneous presence of two signals (liquid- and solid-type) in the range +20 to −60 °C, both corresponding to dispersed Cu(II) ions in amorphous water matrices, can only be interpreted in terms of two sets of correlation times.

Since Cu(II) ions directly bonded to surface sites are excluded from the considerations of the previous sections, the only plausible explanation is that part of the Cu(II) ions resides in a highly immobilized region, that must be obviously identified with the first layers of water molecules, whose mobility is strongly reduced by the attractive forces. If this is true, the correlation times for Cu(II) ion in the immobilized water should not be shorter than $\sim 10^{-8}$ s at room temperature. With decreasing temperatures both the immobilized region and the free water decrease their mobility and more intensity is transferred toward the immobilized region, until all water behaves as a glassy matrix in the ESR time scale. This happens below ∼−70 °C.

At room temperature, the immobilization effect should be confined to no more than two or three layers as suggested by calorimetric data.[29] In fact, in S4, and in S6 also (whose be-

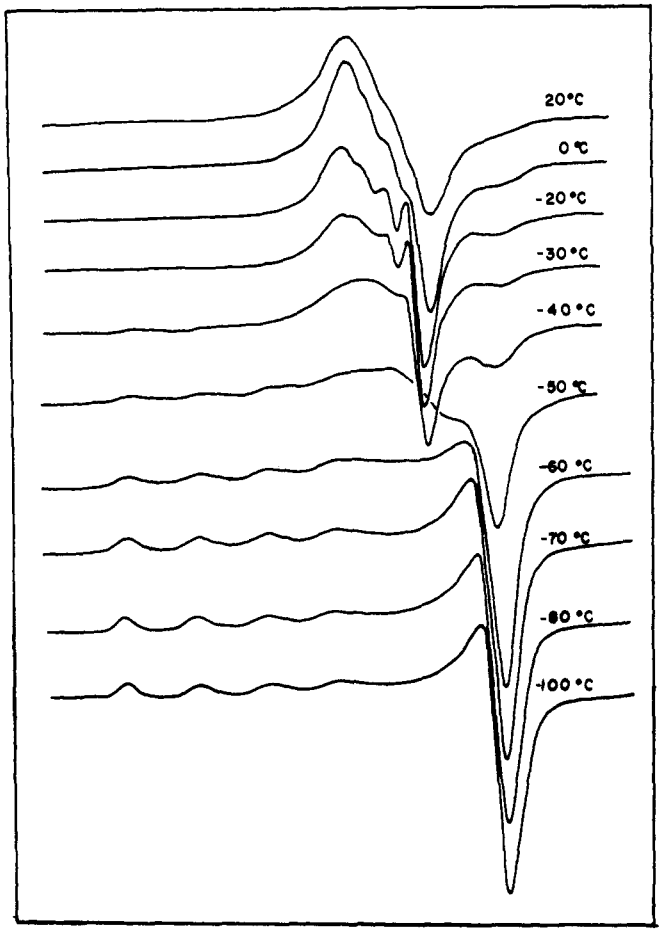

Figure 6. ESR spectra of $Cu(H_2O)_6^{2+}$ aqueous solution adsorbed on S4 as a function of temperature in the range 20 to −100 °C.

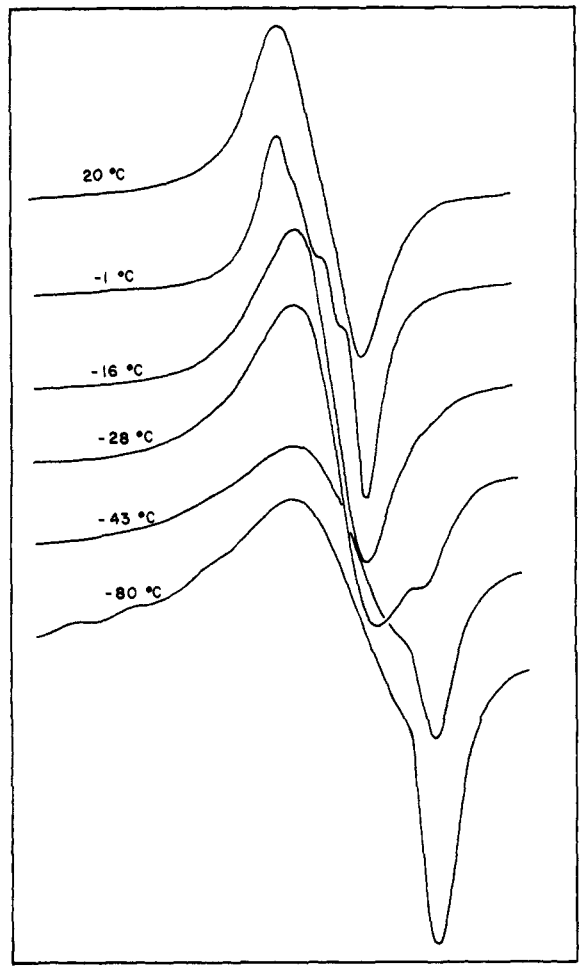

Figure 7. ESR spectra of $Cu(H_2O)_6^{2+}$ aqueous solution adsorbed on S100 as a function of temperature in the range 20 to −80 °C.

havior is similar to that of S4), the first two layers of water molecules contain about 35 and 25% of the total water content. The boundary layer between the two regions is certainly not well defined and we only state that strong immobilization is induced by short range immobilization at the liquid-solid interface.

The actual situation could be represented by a different degree of mobility which leads to reorientational correlation times from $\lesssim 10^{-8}$ (first two or three layers, solid-type spectrum) to $\sim 11^{-11}$ s (innermost layers, liquid-type spectrum). These values of the correlation times depend on temperature as expected and the distribution may be maintained even at low temperature, with the lower values higher, however, than 10^{-8} s, with a resultant glassy spectrum for all Cu(II) ions in the cavities.

Figure 7 shows the temperature dependence of Cu(II) spectra in the S100 sample. In this case, no background signal is observed at room temperature. Only below −15 to −20 °C the glassy spectrum A appears together with the broad signal G (see Figure 4). At −80 °C the signal is almost the same as at 77 K. S20 and S50 samples behave in an intermediate way between S4 and S100; the temperatures of disappearance of the liquid spectrum increase with the increase of the pore diameter. The opposite is found for the appearance of the glassy spectrum. The above observations agree with the increasingly lower content of water molecules in the first layers of adsorbed water (~7, ~3, and ~1% of the total amount of water are involved in the first two layers in S20, S50, and S100, respectively). The region of immobilized water is therefore more and more restricted with respect to the extent of the free region. The ESR spectra of Cu(II) ions in the layers immediately adjacent to the surface escape observation at room temperature because of their very low intensity.

Figure 8 shows the DSC diagrams of silica samples with adsorbed solutions and that of pure water. From these diagrams we may observe that (a) the enthalpy changes are initially spread over a large field of temperature (from −40 to −30 to −12 to −8 °C depending on the samples) and drop abruptly at rather well defined temperatures (−10 to −5 °C), in the cases of silicas with pore diameters >6 nm; (b) in the S4 and S6 samples only the largely spread enthalpy change (from −80 to −60 to −18 to −15 °C) is observed without sharp decrease of the DSC diagram line at the higher temperatures.

The ΔQ changes, measured from the water content in fully hydrated samples, are significantly lower than the ΔQ of pure water.

The lower values of the enthalpy change ranges correspond fairly well with those of disappearance of the liquid-type ESR spectra.

In order to exclude any influence of the Cu(II) ion in the freezing behavior, the DSC experiments were repeated with ion-free water adsorption and identical results were obtained.

Interpreting this set of results it is possible to state that (1) the presence of the glassy-type spectrum A indicates that amorphous solid water is formed upon freezing (*unfreezable water*); (2) the presence of polycrystalline spectrum G indicates that part of the water filling the pores undergoes crystallization (*freezable water*); (3) the spread enthalpy changes and the sharp peak in the DSC diagrams must be correlated with the presence of unfreezable and freezable water in the supports; the first two to three layers of immobilized water molecules are expected to give small variations in the ΔQ.[29]

Anomalous behavior of water in silica gel pores was observed

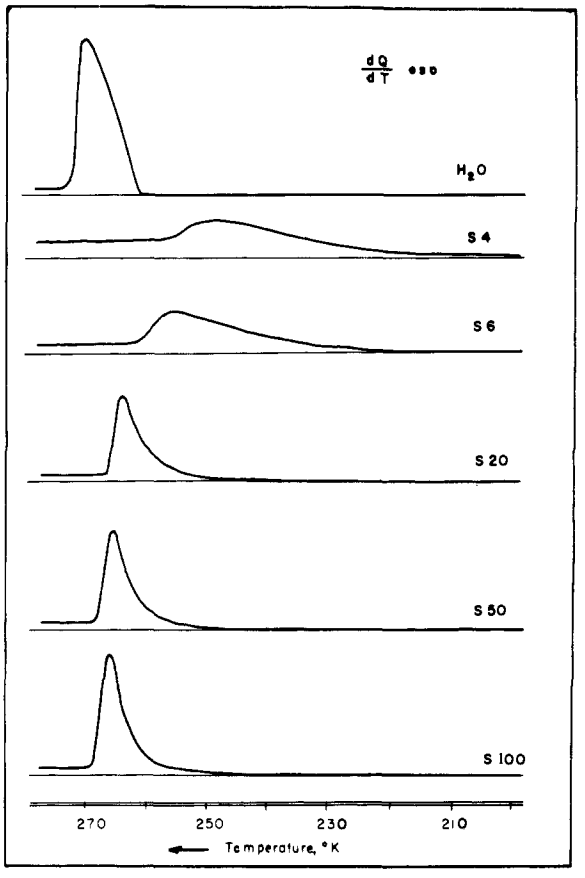

Figure 8. DSC diagrams of free water and of water solutions adsorbed on silica gels.

in many cases[1] and several mechanisms for the interaction of adsorbed water molecules with the silica surface were advanced.[30-34] For instance, Prigogine and Fripiat[34] proposed that the strong donor property of the -OH surface groups and the low basicity of the oxygen atoms in the Si-O-Si bridges would provide the polarizing effects necessary to establish a long-range order, with a change of the physical properties of the adsorbed molecules. It was reported that the first two water layers adsorbed on porous supports show, at 27 °C, an apparent heat capacity that is considerably higher than that of liquid bulk water.[29,35] This fact was attributed to the different structure of the water in the first two layers. The water molecules in this region have coordination numbers lower than those in bulk liquid and therefore the vibrational freedom is substantially increased. Further condensation is influenced by the first layers and results in a modified structure of the adsorbate which does not undergo crystallization.

Proton relaxation measurements of adsorbed water were mainly carried out on systems with only a few layers of adsorbed water molecules.[36-39] The results have indicated that the mean viscosity of this water is higher than that of free water (one to three orders of magnitude depending on the support and on the degree of coverage) although significantly lower (four to two orders of magnitude) than that of ice. The apparent discrepancies between ESR and NMR data arise from the fact that paramagnetic probes require multilayer coverage in which the probe is able to move and thus is somewhat far away from the surface, while proton resonance normally gives results over *all* water protons belonging to any layers.

As reported above, ESR and DSC results show that the smaller the pore diameter, the less complete is the crystallization of the water filling the pores. Since only in the S4 samples no freezable water was found from both ESR and DSC, and assuming the silica gel samples to be strictly homoporous, it may be stated that unfreezable water extends through at least the first ~ten layers. The usual ice structure cannot be formed in this region and a relatively high mobility is retained by the water molecules even at temperatures below −40 to −41 °C, which has been suggested to be the temperature of homogeneous nucleation of water.[40]

Freezable water must therefore involve the water molecules whose distance from the surface is higher than 2 nm, i.e., in pores larger than 4 nm. In these pores a higher number of layers can be accommodated (up to 250 in S100) and the unfreezable water fraction in the first ten layers from the surface progressively decreases from ~85% in S6 to ~7% in S100 of the total water in the pore. The observed ESR intensity of the crystal-type spectrum G (see Figure 4), which is due to Cu(II) ions dissolved in water undergoing crystallization, is strictly correlated to the freezable water fraction. In these samples a structure similar to that of ice can be formed at temperature not far from 0 °C with normal segregation of Cu(II) salt crystals which give rise to the broad signal. Depressions of the freezing point of water adsorbed on porous supports have been widely observed in the past. This effect was attributed to long-range meniscus effects inducing a structure variation even in the middle of the capillary.[29,41,42] The innermost layers of water cannot therefore be strictly considered as true bulk water but rather as a set of separate domains as a consequence of the different structure of the water.

Pearson and Derbyshire,[36] in a proton relaxation study of water adsorbed on silicas of different porosities, observed freezable and unfreezable water. The former type was suggested to be present when the pore diameter was higher than 3-12 nm with the lower value assumed as preferable. The ESR and DSC data reported in this work agree fairly well with this suggestion. In the used samples, this range should be restricted to 4-6 nm since in S6 the amount of freezable water, as can be determined by a qualitative inspection in the ESR patterns at 77 K, is appreciable again.

Acknowledgments. Thanks are due to the Italian National Council of Research (CNR) for the financial support.

References and Notes

(1) J. Clifford in "Water—a Comprehensive Treatise", Vol. V, F. Franks, Ed., Plenum Press, New York, 1975, pp 75-132.
(2) A. C. Zettlemoyer, F. J. Micale, and K. Klier in ref 1, pp 249-291.
(3) H. A. Resing, *Adv. Mol. Relaxation Processes*, 1, 109 (1967).
(4) J. J. Fripiat, *Catal. Rev.*, **5**, 269 (1971).
(5) M. J. Tait and F. Franks, *Nature (London)*, **230**, 91 (1971).
(6) M. L. Hair, "Infrared Spectroscopy in Surface Chemistry", Arnold, London, 1967.
(7) L. Burlamacchi, *J. Chem. Soc., Faraday Trans. 2*, **71**, 54 (1975).
(8) L. Burlamacchi, G. Martini, and M. F. Ottaviani, *J. Chem. Soc., Faraday Trans. 2*, **72**, 324 (1976).
(9) N. N. Tikhomirova, I. V. Nikolaeva, E. N. Rosolovskaya, V. V. Demkin, and K. V. Topchieva, *J. Catal.*, **40**, 61 (1975).
(10) W. B. Lewis and L. O. Morgan in "Transition Metal Chemistry", Vol. IV, R. L. Carlin, Ed., Marcel Dekker, New York, 1968, p 33.
(11) L. Burlamacchi, G. Martini, M. F. Ottaviani, and M. Romanelli, *Adv. Mol. Relaxation Processes*, **12**, 145 (1978); M. Romanelli and L. Burlamacchi, *Mol. Phys.*, **31**, 115 (1976).
(12) R. Poupko and Z. Luz, *J. Chem. Phys.*, **57**, 3311 (1971).
(13) W. B. Lewis, M. Alei, Jr., and L. O. Morgan, *J. Chem. Phys.*, **44**, 2409 (1966).
(14) D. Kivelson, *J. Chem. Phys.*, **41**, 1904 (1964).
(15) R. Wilson and D. Kivelson, *J. Chem. Phys.*, **44**, 154 (1966).
(16) P. W. Atkins and D. Kivelson, *J. Chem. Phys.*, **44**, 169 (1966).
(17) W. B. Lewis, M. Alei, Jr., and L. O. Morgan, *J. Chem. Phys.*, **45**, 4003 (1966).
(18) M. Noack, G. F. Kokoszka, and G. Gordon, *J. Chem. Phys.*, **54**, 1342 (1971).
(19) W. W. Schmidt and K. G. Breitschwert, *Chem. Phys. Lett.*, **27**, 527 (1974).
(20) R. Wilson, Thesis, University of California at Berkeley, 1975.
(21) G. Martini and L. Burlamacchi, *Chem. Phys. Lett.*, **41**, 129 (1976).
(22) J. B. Spencer, Thesis, University of California at Berkeley, 1965.
(23) J. Turkevich, *Catal. Rev.*, 1, 1 (1968).
(24) J. H. Freed, G. V. Bruno, and C. F. Polnaszek, *J. Phys. Chem.*, **75**, 3385 (1971).
(25) C. F. Polnaszek, G. V. Bruno, and J. H. Freed, *J. Chem. Phys.*, **58**, 3185 (1973).
(26) D. Kivelson and R. Neiman, *J. Chem. Phys.*, **35**, 149 (1961).

(27) A. H. Maki and B. R. McGarvey, *J. Chem. Phys.*, **29**, 31 (1958).
(28) See, for instance, B. A. Goodman and J. B. Raynor, *Adv. Inorg. Chem. Radiochem.*, **13**, 135 (1970).
(29) A. A. Antoniou, *J. Phys. Chem.*, **68**, 2754 (1964).
(30) O. Y. Samoilov, *Zh. Fiz. Khim.*, **20**, 12 (1946).
(31) E. Forslind, *Proc. Int. Congr. Rheol., 2nd*, 50 (1953).
(32) H. S. Franks and W. Y. Wen, *Discuss. Faraday Soc.*, **24**, 133 (1957).
(33) M. Prigogine and J. J. Fripiat, *Chem. Phys. Lett.*, **12**, 107 (1971).
(34) M. Prigogine and J. J. Fripiat, *Bull. Soc. R. Sci. Liege*, **43**, 449 (1974).
(35) G. F. C. Frohnsdorff and G. L. Kington, *Proc. R. Soc. London, Ser. A*, **274**, 469 (1958).
(36) R. T. Pearson and W. Derbyshire, *J. Colloid Interface Sci.*, **46**, 232 (1974).
(37) H. A. Resing, *J. Phys. Chem.*, **78**, 1279 (1974).
(38) G. Belfort, J. Sherfig, and D. O. Seevers, *J. Colloid Interface Sci.*, **47**, 106 (1974).
(39) H. A. Resing and J. K. Thomson, *Adv. Chem. Ser.*, **101**, 473 (1971).
(40) D. H. Rasmussen and A. P. Mac Kenzie in "Water Structure at the Water-Polymer Interface", H. H. G. Jellinek, Ed., Plenum Press, New York, 1972, p 126.
(41) A. R. Ubbelohde, *Q. Rev., Chem. Soc.*, **4**, 356 (1950).
(42) C. Hodgson and R. McIntosh, *Can. J. Chem.*, **38**, 958 (1960).

Free Energies of Solution of Rare Gases and Alkanes in Water and Nonaqueous Solvents. A Quantitative Assessment of the Hydrophobic Effect

Michael H. Abraham

Contribution from the Department of Chemistry, University of Surrey, Guildford, Surrey, United Kingdom. *Received July 3, 1978*

Abstract: Standard free energies of solution of the rare gases and alkanes in water and in over 16 nonaqueous solvents are tabulated. It is shown that it is difficult to reach unambiguous conclusions about the existence of the hydrophobic effect from plots of $\Delta G_s°$ against solute radius or solute volume, partly because of inherent uncertainties in the values of the solute radius. It is found that $\Delta G_s°$ values for both rare gases and alkanes in all nonaqueous solvents are well correlated through linear equations: $\Delta G_s°(\text{solvent}) = m\Delta G_s°(\text{benzene}) + c$ and $\Delta G_s°(\text{solvent}) = lR + d$, where R is a solute parameter related to solute radius. When applied to $\Delta G_s°$ values for solution in water, these equations show conclusively that the solution of alkanes (but not rare gases) in water is quite anomalous. The $-CH_2-$ increment for partition of *n*-alkanes between hexane and water is 0.92 kcal mol^{-1} in favor of hexane, and can be separated into a favorable gas → hexane contribution of 0.74 kcal mol^{-1} and an unfavorable gas → water contribution of 0.18 kcal mol^{-1}. The latter is further dissected into a true (unfavorable) hydrophobic contribution of 0.54 kcal mol^{-1} and a favorable normal solvent effect of 0.36 kcal mol^{-1}. Methods for the estimation and prediction of $\Delta G_s°$ values in nonaqueous solvents are discussed.

Liszi and I have tabulated data on the free energy of solution of rare gases and the lower alkanes in a variety of solvents.[1] We observed that, when the $\Delta G_s°$ values for a series of solutes in a given solvent were plotted against the solute radius, reasonable straight lines were obtained for every solvent studied except water. In the latter case, a straight line was found only for solution of the rare gases and it was suggested[1] that the solution of alkanes in water gave rise to anomalous free energies. While this work was in the press, Cramer[2] showed that, when $\Delta G_s°$ values for rare gases and *n*-alkanes in water and 1-octanol were plotted against solute molecular volume, quite similar patterns of behavior were observed for the two solvents. Cramer[2] concluded that the mechanism of solvation of the above solutes by water and 1-octanol was fundamentally similar and hence that prevailing descriptions of the hydrophobic effect could not be correct.

It is obviously of great importance to establish whether or not water is unique with respect to the solution of hydrocarbons, and I thought it useful to assemble results on the free energy of solution of rare gases and an extended series of alkanes, and to explore the observed patterns of the $\Delta G_s°$ values. The latter are expressed as standard free energies of solution in kcal mol^{-1}, and refer to the process

$$\text{solute (gas, 1 atm)} \rightarrow \text{solute (solution, unit mole fraction)} \quad (1)$$

Values for the rare gases and the C_1 to C_4 alkanes in water are from the review by Wilhelm, Battino, and Wilcock;[3] those for solution of the higher *n*-alkanes in water are from results compiled by Hine and Mookerjee.[4] Data on the rare gases in nonaqueous solvents are mainly from the work of Battino et al.,[5] supplemented by values given by de Ligny et al.[6] and by Linford and Thornhill.[7] For the rare gases in methanol, the results of Beckwith and of Law were used.[8] Numerous workers[9-25] have reported data from which were calculated $\Delta G_s°$ values for alkanes in nonaqueous solvents. Values of $\Delta G_s°$ for the rare gases and *n*-alkanes in various solvents are in Table I, together with values for solvent 1-octanol, used by Cramer.[2]

Inspection of Table I shows that, for any given nonaqueous solvent, $\Delta G_s°$ decreases with increasing solute size. This trend is not easy to quantify, because there is no unambiguous measure of solute size for the nonelectrolytes involved. In Table II are given some values of solute radii (Å) used by various workers. The rare gas radii used by Abraham and Liszi[1] were taken from Huheey[26] and differ considerably from those used by Cramer,[2] taken from the work of Bondi.[27] Other sets of rare-gas radii[6,28] agree with those used by Abraham and Liszi, but yet others[29] are close to those used by Cramer. It seems clear that any analysis of $\Delta G_s°$ values and solute size will suffer from the inherent difficulty of assigning solute radii (and hence molecular volume). This is illustrated in Figures 1 and 2, where are given plots of $\Delta G_s°$ for rare gases and C_1 to C_5 *n*-alkanes in benzene, 1-octanol, and water against solute radius; in Figure 1 are used the radii of Abraham and Liszi and in Figure 2 the radii of Cramer are used. Although there is considerable scatter, especially in Figure 1, a fairly straight line can be drawn through all the points in benzene and in 1-octanol. The discrepancies, although apparently quite large, are actually within the uncertainty in solute radius. This can be demonstrated by the construction of a set of solute radii, R, designed so that plots of $\Delta G_s°$ against R yield straight lines for the case of the nonaqueous solvents. These constructed radii are in

0002-7863/79/1501-5477$01.00/0